JAMES | Journal of Advances in Modeling Earth Systems

RESEARCH ARTICLE
10.1029/2018MS001549

Special Section:
Community Earth System Model version 2 (CESM2) Special Collection

A Total Energy Error Analysis of Dynamical Cores and Physics-Dynamics Coupling in the Community Atmosphere Model (CAM)

Peter H. Lauritzen[1] **and David L. Williamson**[1]

[1]National Center for Atmospheric Research, Boulder, CO, USA

Key Points:
- Spurious total energy dissipation in dynamical core is -0.3 W/m^2 to -1 W/m^2 at 1 deg
- Constant-pressure assumption in physics leads to 0.3 W/m^2 spurious total energy source
- There can easily be compensating errors in total energy budget

Correspondence to:
P. H. Lauritzen,
pel@ucar.edu

Citation:
Lauritzen, P. H., & Williamson, D. L. (2019). A total energy error analysis of dynamical cores and physics-dynamics coupling in the Community Atmosphere Model (CAM). *Journal of Advances in Modeling Earth Systems*, *11*, 1309–1328. https://doi.org/10.1029/2018MS001549

Received 2 NOV 2018
Accepted 5 FEB 2019
Accepted article online 7 FEB 2019
Published online 9 MAY 2019

Abstract A closed total energy (TE) budget is of utmost importance in coupled climate system modeling; in particular, the dynamical core or physics-dynamics coupling should ideally not lead to spurious TE sources/sinks. To assess this in a global climate model, a detailed analysis of the spurious sources/sinks of TE in National Center for Atmospheric Research's Community Atmosphere Model (CAM) is given. This includes spurious sources/sinks associated with the parameterization suite, the dynamical core, TE definition discrepancies, and physics-dynamics coupling. The latter leads to a detailed discussion of the pros and cons of various physics-dynamics coupling methods commonly used in climate/weather modeling.

1. Introduction

In coupled climate modeling with prognostic atmosphere, ocean, land, land-ice, and sea-ice components, it is important to conserve total energy (TE) to a high degree in each component individually and in the complete model to avoid spurious long-term trends in the simulated Earth system. Conservation of TE in this context refers to having a closed TE budget. For example, the TE change in a column in the atmosphere is exactly balanced by the net sources/sinks given by the fluxes through the column. The fluxes into the atmospheric component from the surface models must be balanced by the fluxes in the respective surface components and so on. Henceforth, we will focus only on the atmospheric component which, in a numerical model, is split into a resolved-scale component (the dynamical core) and a subgrid-scale component (parameterizations or, in modeling jargon, physics). While there have been many studies on energy flow in the Earth system through analysis of reanalysis data and observations (Trenberth & Fasullo, 2018, and references therein), there has been less focus on spurious TE sources/sinks in numerical models.

The atmospheric equations of motion conserve TE, but the discretizations used in climate and weather models are usually not inherently TE conservative. Exact conservation is probably not necessary but conservation to within ~0.01 W/m^2 has been considered sufficient to avoid spurious trends in century long simulations (Boville, 2000; Williamson et al., 2015). Spurious sources and sinks of TE can be introduced by the dynamical core, physics, physics-dynamics coupling (PDC), and discrepancies between the TE of the continuous and discrete equations of motion and for the physics. Hence, the study of TE conservation in comprehensive models of the atmosphere quickly becomes a quite complex and detailed matter. In addition there can easily be compensating errors in the system as a whole.

Here we focus on versions of the Community Atmosphere Model (CAM) that use the spectral-element (SE; Lauritzen et al., 2018) and finite-volume (FV; Lin, 2004) dynamical cores. These dynamical cores couple with physics in a time-split manner; that is, physics receives a state updated by dynamics (see Williamson, 2002, for a discussion of time-split versus process split PDC in the context of CAM). In its pure time-split form the physics tendencies are added to the state previously produced by the dynamical core and the resulting state provides the initial state for the subsequent dynamical core calculation. We refer to this as *state-updating* (`ftype=1` in CAM code). Alternatively, when the dynamical core adopts a shorter time step than the physics, say `nsplit` substeps, then (1/`nsplit`)th of the physics-calculated tendency is added to the state before each dynamics substep. We refer to this modification of time splitting as dribbling (`ftype=0`). CAM-FV uses the *state update* (`ftype=1`) approach while CAM-SE has options to use *state update* (`ftype=1`), *dribbling* (`ftype=0`), or a combination of the two, that is, mass variables use *state-updating* and remaining variables use *dribbling*. We refer to this as *combination* (`ftype=2`). The

dribbling variants can lead to spurious sources or sinks of TE (and mass) referred to here as PDC errors. Any error in the water mass budget associated with dribbling affects the mass-weightening in the TE integral and hence introduces TE errors.

The dynamical core usually has inherent or specified filters to control spurious noise near the grid scale which will lead to energy dissipation (Jablonowski & Williamson, 2011; Thuburn, 2008). Similarly, models often have sponge layers to control the solution near the top of the model that may be a sink of TE. There are examples of numerical discretizations of the adiabatic frictionless equations motion that are designed so that TE is conserved in the absence of time-truncation and filtering errors, for example, mimetic spectral-element discretizations such as the one used in the horizontal in CAM-SE (Eldred & Randall, 2017; McRae & Cotter, 2013; Taylor, 2011). These provide consistency between the discrete momentum and thermodynamic equations leading to global conservation associated with the conversion of potential to kinetic energy. In spectral transform models it is customary to add the energy change due to explicit diffusion on momentum back as heating (referred to as frictional heating), so that the diffusion of momentum does not affect the TE budget (see, e.g., p.71 in Neale et al., 2012). This is also done in CAM-SE (Lauritzen et al., 2018).

The purpose of this paper is to provide a detailed global TE analysis of CAM. We assess TE errors due to various steps in the model algorithms. The paper is outlined as follows. In section 2 the continuous TE formulas are given and a detailed description of spurious TE sources/sinks that can occur in a model as a whole, and the associated diagnostics used to perform the TE analysis, are defined. In section 3 the model is run in various configurations to assess their effects on TE conservation. This includes various PDC experiments leading to a rather detailed discussion of mass budget closure. We also investigate the effect of using a limiter in the vertical remapping of momentum, assess energy discrepancy errors and impacts on TE of simplifying surface conditions and dry atmosphere experiments. The paper ends with conclusions.

2. Method

2.1. Defining TE

In the following it is assumed that the model top and bottom are coordinate surfaces and that there is no flux of mass through the model top and bottom. In a dry hydrostatic atmosphere the TE equation integrated over the entire sphere is given by

$$\frac{\mathrm{d}}{\mathrm{d}t}\int_{z=z_s}^{z=z_{top}}\iint_S E_v\rho^{(d)}\,\mathrm{d}A\,\mathrm{d}z = \int_{z=z_s}^{z=z_{top}}\iint_S F_{net}\,\rho^{(d)}\mathrm{d}A\,\mathrm{d}z, \tag{1}$$

(e.g., Kasahara, 1974) where F_{net} is net flux calculated by the parameterizations (e.g., heating and momentum forcing), $\mathrm{d}/\mathrm{d}t$ the total/material derivative, z_s is the height of the surface, S the sphere, $\rho^{(d)}$ the density of dry air, E_v is the TE and $\mathrm{d}A$ is an infinitesimal area on the sphere. E_v can be split into kinetic energy $K = \frac{1}{2}\mathbf{v}^2$ ($\mathbf{v}$ is the wind vector), internal energy $c_v^{(d)}T$, where $c_v^{(d)}$ is the heat capacity of dry air at constant volume, and potential energy $\Phi = gz$

$$E_v = K + c_v^{(d)}T + \Phi. \tag{2}$$

If the vertical integral is performed in a mass-based vertical coordinate, for example, pressure, then the integrated TE equation for a dry atmosphere can be written as

$$\frac{d}{\mathrm{d}t}\int_{p=p_s}^{p=p_{\mathrm{top}}}\iint_S E_p\,\mathrm{d}A\,\mathrm{d}p + \frac{\mathrm{d}}{\mathrm{d}t}\iint_S \Phi_s p_s \mathrm{d}A = \int_{p=p_s}^{p=p_{\mathrm{top}}}\iint_S F_{\mathrm{net}}\,\mathrm{d}A\,\mathrm{d}p, \tag{3}$$

(e.g., Kasahara, 1974) where

$$E_p = K + c_p^{(d)}T. \tag{4}$$

In a moist atmosphere, however, there are several definitions of TE used in the literature related to what heat capacity is used for water vapor and whether or not condensates are accounted for in the energy equation. To explain the details of that, we focus on the energy equation for CAM-SE.

CAM-SE is formulated using a terrain-following hybrid-sigma vertical coordinate η but the coordinate levels are defined in terms of dry air mass per unit area ($M^{(d)}$) instead of total air mass; $\eta^{(d)}$ (see Lauritzen et al., 2018, for details). In such a coordinate system it is convenient to define the tracer state in terms of a dry mixing ratio instead of moist mixing ratio

$$m^{(\ell)} \equiv \frac{\rho^{(\ell)}}{\rho^{(d)}}, \text{where } \ell = \text{'}wv\text{'}, \text{'}cl\text{'}, \text{'}ci\text{'}, \text{'}rn\text{'}, \text{'}sw\text{'}, \tag{5}$$

where $\rho^{(d)}$ is the mass of dry air per unit volume of moist air and $\rho^{(\ell)}$ is the mass of the water substance of type ℓ per unit volume of moist air. Moist air refers to air containing dry air ('*d*'), water vapor ('*wv*'), cloud liquid ('*cl*'), cloud ice ('*ci*'), rain amount ('*rn*'), and snow amount ('*sw*'). For notational purposes define the set of all components of air

$$\mathcal{L}_{\text{all}} = \{\text{'}d\text{'}, \text{'}wv\text{'}, \text{'}cl\text{'}, \text{'}ci\text{'}, \text{'}rn\text{'}, \text{'}sw\text{'}\}, \tag{6}$$

Define associated heat capacities at constant pressure $c_p^{(\ell)}$. We refer to condensates as being thermodynamically and inertially active if they are included in the thermodynamic equation and momentum equations; for example, if the thermodynamic equation is formulated in terms of temperature, the energy conversion term includes a generalized heat capacity which is a function of the condensates and their associated heat capacities (see, e.g., section 2.3 in Lauritzen et al., 2018). Similarly, the weight of the condensates is included in the pressure field and pressure gradient force. How many condensates are thermodynamically/inertially active in the dynamical core, and which is controlled with namelist `qsize_condensate_loading`. If `qsize_condensate_loading = 1`, only water vapor ('*wv*') is active, `if qsize_condensate_loading = 3`, '*wv*,' '*cl*,' and '*ci*' are active, and if `qsize_condensate_loading = 5`, then '*wv*,' '*cl*,' '*ci*,' '*rn*,' and '*sw*' are included.

Using the $\eta^{(d)}$ vertical coordinate and dry mixing ratios the TE (per unit area) that the frictionless adiabatic equations of motion in the CAM-SE dynamical core conserves is

$$\widehat{E}_{\text{dyn}} = \frac{1}{\Delta S}\int_{\eta=0}^{\eta=1}\iint_S \left(\frac{1}{g}\frac{\partial M^{(d)}}{\partial \eta^{(d)}}\right)\sum_{\ell\in\mathcal{L}_{\text{all}}}\left[m^{(\ell)}\left(K + c_p^{(\ell)}T + \Phi_s\right)\right]\mathrm{d}A\mathrm{d}\eta^{(d)}, \tag{7}$$

where ΔS is the surface area of the sphere, Φ_s is the surface geopotential, and $\widehat{(\cdot)}$ refers to the global average.

In the CAM physical parameterizations a different definition of TE is used. Due to the evolutionary nature of the model development, the parameterizations have not yet been converted to match the SE dynamical core. For the computation of TE, condensates are assumed to be zero and the heat capacity of moisture is the same as for dry air. This is equivalent to using a moist mass (dry air plus water vapor) but c_p of dry air

$$\widehat{E}_{\text{phys}} = \frac{1}{\Delta S}\int_{\eta=0}^{\eta=1}\iint_S \left(\frac{1}{g}\frac{\partial M^{(d)}}{\partial \eta^{(d)}}\right)\left(1 + m^{(wv)}\right)\left[\left(K + c_p^{(d)}T + \Phi_s\right)\right]\mathrm{d}A\mathrm{d}\eta^{(d)}. \tag{8}$$

We note that earlier versions of CAM using the spectral transform dynamical core used c_p of moist air. The adiabatic, frictionless equations of motion in the CAM-SE dynamical core can be made consistent with E_{phys} by not including condensates in the mass/pressure field as well as energy conversion term in the thermodynamic equation and setting the heat capacity for moisture to $c_p^{(d)}$ (Taylor, 2011). We refer to this version of CAM-SE combined with *state-updating* (`ftype=1`) PDC as the *energy consistent* version; that is, the same continuous formula for energy is used in both dynamics and physics, and there are no PDC errors.

2.2. Some Remarks on Local Energy Conservation

Although this paper focuses on global average TE errors, it is important to note that energy errors occur locally. For example, when an air parcel gains or loses water via evaporation or precipitation (or via a fixer or borrower to maintain some physical property like positive definiteness), there are implications for the mass, heat content, and heat capacity of the parcel. In turn, that affects the energy and mass of the column and thereby affects the global TE budget. So anything that changes these state variables locally has implications for the TE budget.

An example of an inconsistency in CAM physics is that surface pressure is held fixed during physical parameterization updates, but water vapor, and hence surface pressure, does change during evaporation/precipitation and an inconsistency appears in the mass and energy budget (see item 2 in section 2.3).

Similarly, if a "clipper" is used on water vapor or condensates to avoid (unphysical) negative mixing ratios (more details in section 3.2) and this is not accounted for in the thermodynamics or through a surface flux, that "clipping" will produce an energy source via the mass weightening in the TE vertical integral. In the dynamical core TE is not conserved locally in each column as there is a horizontal flux of energy between columns; but the local energy budget should, ideally, be closed and thereby, globally, TE should be conserved. If a dynamical core does not inherently conserve dry air mass and/or water mass then a spurious source of TE is inevitable again through the mass weightening in the vertical integral (unless fixers are applied).

2.3. Spurious Energy Sources and Sinks

In a weather/climate model TE conservation errors can appear in many places throughout the algorithm. Below is a general list of where conservation errors can appear with specific examples from CAM:

1. *Parameterization errors*: Individual parameterizations may not have a closed energy budget; for example, they may not have been designed to conserve the discrete TE as defined in the model or they may conserve a discrete TE defined differently. CAM parameterizations are required to have a closed energy budget (based on the discrete TE definition in CAM) under the assumption that pressure remains constant during the computation of the subgrid-scale parameterization tendencies. In other words, the TE change in the column is exactly balanced by the net sources/sinks given by the fluxes through the column (If not, a fixer needs to be applied since the CAM global TE fixer as implemented does not include any errors from the parameterizations. For example, in CAM parameterizations occasionally produce negative water vapor. These are filled without compensation and therefore affect the TE, but errors tend to be small.).
2. *Pressure work*: That said, if parameterizations update specific humidity then the surface pressure changes (e.g., moisture entering or leaving the column). In that case the pressure changes which, in turn, changes TE. This is referred to as *pressure work* (section 3.1.8 in Neale et al., 2012).
3. *Continuous TE formula discrepancy*: If the continuous equations of motion for the dynamical core conserve a TE different from the one used in the parameterizations then an energy inconsistency is present in the system as a whole. This is the case with the new version of CAM-SE that conserves a TE that is more accurate and comprehensive than that used in the CAM physics package as discussed above. As also noted above, this mismatch arose from the evolutionary nature of the model development and not by deliberate design; and should be eliminated in the future.
4. *Dynamical core errors*: Energy conservation errors in the dynamical core, not related to PDC errors, can arise in multiple parts of the algorithms used to solve the equations of motion. For dynamical cores employing filtering (e.g., limiters in flux operators, Lin, 2004) and/or possessing inherent damping which controls small scales, it is hard to isolate their energy dissipation from other errors in the discretization. If a hyperviscosity term or some other diffusion is added to the momentum equation, then one can diagnose the local energy dissipation from such damping and add a corresponding heating to balance it (frictional heating). There may also be energy loss from viscosity applied to other variables such a temperature or pressure which is harder to compensate. Here is a breakdown relevant to CAM-SE using a floating Lagrangian vertical coordinate:
   - Horizontal inviscid dynamics: Energy errors resulting from solving the inviscid, adiabatic equations of motion.
   - Hyperviscosity: Filtering errors.
   - Vertical remapping: The vertical remapping algorithm from Lagrangian to Eulerian reference surfaces does not conserve TE.
   - Near round-off negative values of water vapor which are filled to a minimal value without compensation.

   If a dynamical core is not inherently mass conservative with respect to dry air, water vapor, and condensates, then TE conservation is affected since

$$\int_{\eta=0}^{\eta=1} \iint_S \left(\frac{1}{g}\frac{\partial M^{(d)}}{\partial \eta^{(d)}}\right) \sum_{\ell \in \mathcal{L}_{\text{all}}} \left[m^{(\ell)}\right] \mathrm{d}A \mathrm{d}\eta^{(d)} \tag{9}$$

   is not conserved. Henceforth, we assume that the dynamical core is based on an inherently mass-conservative formulation which is the case for CAM-SE, CAM-SE-CSLAM (Conservative Semi-LAgrangian Multi-tracer), and CAM-FV.

5. *Physics-dynamics coupling (PDC)*: Assume that physics computes a tendency. Usually the tendency (forcing) is passed to the dynamical core which is responsible for adding the tendencies to the state. PDC energy errors can be split into three types:
   - *"Dribbling" errors (or, equivalently, temporal PDC errors)*: If the TE increment from the parameterizations does not match the change in TE when the tendencies are added to the state in the dynamical core, then there will be a spurious PDC error. This will not happen with the *state-update* approach in which the tendencies are added immediately after physics and before the dynamical core advances the solution in time. The PDC "dribbling" errors can be split into three contributions:
     Thermal energy dribbling error: PDC errors in temperature tendencies occur because the T-increment (call it ΔT) that the parameterizations prescribe leads to a dry thermal energy change of $\Delta M^{(d)}\Delta T$ which will not match the equivalent dry thermal energy change when the temperature tendency is added in smaller chunks in the dynamical core during the "dribbling" of ΔT. The discrepancy occurs because $\Delta M^{(d)}$ changes during each dynamics time step and hence the thermal energy change due to physics forcing accumulated during the "dribbling" will not equal $\Delta M^{(d)}\Delta T$. This error could possibly be eliminated by using thermal energy forcing instead of temperature increments.
     Kinetic energy dribbling error: Similarly, PDC errors in velocity component forcing increments (Δu, Δv) occur because the dry kinetic energy change of $\Delta M^{(d)}\left[(\Delta u)^2 + (\Delta v)^2\right]$ will not match the equivalent dry kinetic energy change when dribbling velocity component forcing increments (Δu, Δv). It is less clear how to eliminate this error as kinetic energy is a quadratic quantity.
     Mass clipping (affects all TE terms): A similar PDC error for mass variables such as vapor forcing and cloud liquid can occur when the mass tendencies are "dribbled" during the dynamical core integration. The dynamical core transport of mass variables will move mass around in the horizonal and vertical while the "dribbled" physics mass increments are applied in the same location; in that situation a negative mass increment from the parameterizations may be larger than the mass available to remove. This can lead to a spurious source mass if there is logic in the dynamical core preventing mixing ratios/mass to become negative. This is referred to as "clipping" PDC errors, and the process is described/discussed in detail in section 3.2.1. The "clipping" changes the water mass budget without accounting for it in water fluxes or in the thermodynamics and hence lead to TE conservation errors (both kinetic and thermal energy).
   - *Change of vertical grid/coordinate errors*: If the vertical coordinates in physics and in the dynamical core are different, then there can be spurious PDC energy errors even when using the state-update method for adding tendencies to the dynamical core state. For example, many nonhydrostatic dynamical cores (e.g., Skamarock et al., 2012) use a terrain-following height coordinate whereas physics uses pressure.
   - *Change of horizontal grid errors:* If the physics tendencies are computed on a different horizontal grid than the dynamical core, then there can be spurious energy errors from mapping tendencies and/or variables between horizontal grids (e.g., Herrington et al., 2019).
6. *Compensating energy fixers:* To avoid TE conservation errors which could accumulate and ultimately lead to a climate drift, it is customary to apply an arbitrary energy fixer to restore TE conservation. Since the spatial distribution of many energy errors, in general, is not known, global fixers are used. In CAM a uniform increment is added to the temperature field to compensate for TE imbalance from all processes, that is, dynamical core, PDC, TE formula discrepancy, and energy change due to pressure work error.

2.4. Diagnostics

The discrete global averages $\widehat{(\cdot)}$ are computed consistent with the discrete model grid as outlined in section 2.2. of Lauritzen et al. (2014). The TE global average tendency is denoted

$$\partial\widehat{E} \equiv \frac{\mathrm{d}\widehat{E}}{\mathrm{d}t}. \tag{10}$$

By computing the global TE averages $\widehat{E}$ at appropriate places in the model algorithms, we can directly compute $\partial\widehat{E}$ due to various processes (such as viscosity, vertical remapping, PDC, and pressure work error) by differencing $\widehat{E}$ from after and before the algorithm takes place. This has been implemented using CAM history infrastructure by computing column integrals of energy at various places in CAM and outputting the 2-D energy fields. CAM history internally handles accumulation and averaging in time at each horizontal grid point. The global averages are computed externally from the grid point vertical integrals on the history files (stored in double precision). The places in CAM where we compute/capture the grid point vertical

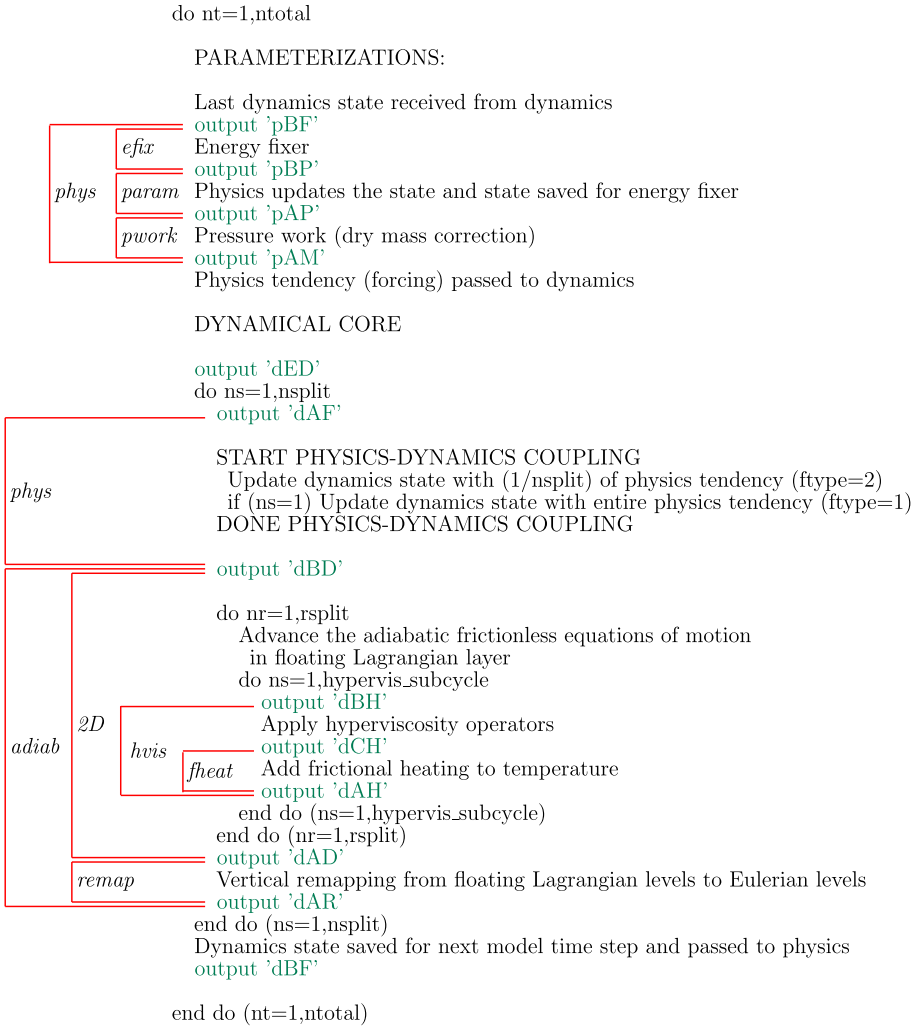

Figure 1. Pseudo-code for CAM-SE showing the order in which relevant physics updates are performed as well as dynamical core steps and associated loops. In green font locations where the state is captured and output is shown together with its three-character identifier. The outermost loop (1, *ntotal*) advances the entire model Δt_{phys} seconds (in this case 1800 s). The dynamical core loops are as follows: the outer loop is the vertical remapping loop (1,`nsplit`) with associated time step Δt_{phys}/`nsplit`. For stability the temporal advancement of the equations of motion in the Lagrangian layer needs to be subcycled `rsplit` times. Within the `rsplit` loop the hyperviscosity time stepping is subcycled *hypervis_subcycle* times (again for stability). For more details on the time stepping in CAM-SE see Lauritzen et al. (2018).

integral E are named using three letters where the first letter refers to whether the vertical integral is performed in physics ("p") or in the dynamical core ("d"). The trailing two letters refer to the specific location in dynamics or physics. For example, "BP" refers to "Before Physics" and "AP" to "After Physics"; the associated total energies are denoted E_{pBP} and E_{pAP}, respectively. The TE tendency from the parameterizations is the difference between E_{pBP} and E_{pAP} divided by the time step. The terms and tendencies are then averaged globally externally to the model. The pseudo-code in Figure 1 defines the acronyms in terms of where in the CAM-SE algorithm the TE vertical integrals are computed and output. For details on the CAM-SE algorithm please see Lauritzen et al. (2018).

Before defining the individual terms in detail we briefly review the model time-stepping sequence starting with the physics component as illustrated in Figure 1. The energy fixer is applied first to compensate for the spurious net energy change from all components introduced during the previous time step. We will describe this in more detail after the various sources and sinks are elucidated. The parameterizations are applied next and are required to be energy conserving. They update the state and accumulate the total physics tendency (forcing). At this stage the state is saved for use in the energy fixer in the next time step. Any changes in

the global average energy after this are spurious and are compensated by the fixer. The parameterizations update the water vapor but not the moist pressure, implying a nonphysical change in the dry mass of the atmosphere. The dry mass correction corrects the dry mass back to its proper value.

The forcing (physics tendency) from the parameterizations is passed to the dynamical core. If the physics and dynamics operate on different grids, the forcing is remapped here. The dynamics operates on a shorter time step than the physics and is substepped. The remapped physics increment is applied to the dynamics state, saved from the end of the previous dynamics step, using either state-updating, dribbling, or combination as described in section 1. The dynamics then advances the adiabatic frictionless flow in the floating Lagrangian layers over a further set of substeps. Hyperviscosity is applied next with further substepping required for computational stability of the explicit discrete approximations. The energy loss from the specified momentum viscosity is calculated locally and is balanced by adding a local change to the temperature, referred to as frictional heating. This set of dynamics substeps is followed by the vertical remapping from Lagrangian to Eulerian reference layers. The remapping is required to provide layers consistent with the parameterization formulations. The vertical remapping substeps are required for stability if the Lagrangian layers become too thin.

At the end of the dynamics, the state is saved to be used by the dynamics the next time step and is also passed to the physics, with a remapping if the dynamics and physics grids differ. At the beginning of the physics the difference in energy between this state and the state saved after the physics during the previous time step is the amount needed to be added or subtracted by the energy fixer. It represents the accumulation of all spurious sources from the dry mass correction, remappings between physics and dynamics grids (if applicable), dynamical core, differing energy definitions (if present), hyperviscosity, and vertical remapping.

We now define the following energy tendencies corresponding to the itemized list in section 2.3 with references to terms indicated in Figure 1. We start just after the energy fixer which will be defined at the end.

1. $\partial\widehat{E}^{(\text{param})}$: TE tendency due to parameterizations. In CAM the TE budget for each parameterization is closed (assuming pressure is unchanged) so $\partial\widehat{E}^{(\text{param})}$ is balanced by net fluxes in/out of the physics columns. Note that this is the only energy tendency that is not spurious since CAM parameterizations have a closed TE budget. This TE tendency is discretely computed as

$$\partial\widehat{E}^{(\text{param})}_{\text{phys}} = \frac{\widehat{E}_{\text{pAP}} - \widehat{E}_{pBP}}{\Delta t_{\text{phys}}}, \tag{11}$$

   where Δt_{phys} is the physics time step (default 1800 s) and the subscript "phys" on $\partial\widehat{E}$ refers to the energy tendency computed in CAM physics. We include the tendency to provide a reference scaling for other errors.
2. $\partial\widehat{E}^{(\text{pwork})}$: Total spurious energy tendency due to pressure work error

$$\partial\widehat{E}^{(\text{pwork})}_{\text{phys}} = \frac{\widehat{E}_{\text{pAM}} - \widehat{E}_{pAP}}{\Delta t_{\text{phys}}}. \tag{12}$$

   Since CAM-SE dynamical core is based on a dry-mass vertical coordinate, the pressure work error takes place implicitly in the dynamical core. But the TE tendency due to pressure work error is conveniently computed in physics since dynamical cores based on a moist vertical coordinate (e.g., CAM-FV) require pressure and moist mixing ratios to be adjusted for dry mass conservation and tracer mass conservation (section 3.1.8 in Neale et al., 2012). The difference of TE after and before this adjustment is the TE tendency due to pressure work error. In a dry mass vertical coordinate based on dry mixing ratios, neither dry mass layer thickness nor dry mixing ratios, need to be adjusted to take into account moisture changes in the column. For labeling purposes, the "total forcing" associated with physics (at least in CAM) consists of parameterizations, pressure work error, and TE fixer, although strictly speaking the fixer includes components from the dynamics as will be seen.

$$\partial\widehat{E}^{(\text{phys})}_{\text{phys}} \equiv \partial\widehat{E}^{(\text{param})}_{\text{phys}} + \partial\widehat{E}^{(\text{pwork})}_{\text{phys}} + \partial\widehat{E}^{(\text{efix})}_{\text{phys}} = \frac{\widehat{E}_{\text{pAM}} - \widehat{E}_{\text{pBF}}}{\Delta t_{\text{phys}}}. \tag{13}$$

where the energy fixer TE tendency is

$$\partial\widehat{E}^{(\mathrm{efix})}_{\mathrm{phys}} = \frac{\widehat{E}_{\mathrm{pBP}} - \widehat{E}_{\mathrm{pBF}}}{\Delta t_{\mathrm{phys}}}. \tag{14}$$

After all the TE budget terms have been defined, the exact composition of $\partial\widehat{E}^{(\mathrm{efix})}_{\mathrm{phys}}$ will be presented.

3. $\partial\widehat{E}^{(\mathrm{discr})}$: If the physics uses a TE definition different from the TE that the continuous equations of motion in the dynamical core conserve (i.e., in the absence of discretization errors), then there is a TE discrepancy tendency. This complicates the energy analysis as one cannot compare TE computed in physics $\widehat{E}_{\mathrm{phys}}$ directly with TE computed in the dynamical core $\widehat{E}_{\mathrm{dyn}}$. This makes errors associated with this discrepancy tricky to assess. That said, the TE tendencies computed using the dynamical core TE formula $\partial\widehat{E}_{\mathrm{dyn}}$ are well defined (self consistent) and similarly for TE tendencies computed using the "physics formula" for TE, $\partial\widehat{E}_{\mathrm{phys}}$.
4. The TE tendency from the dynamical core is split into several terms: Horizontal adiabatic dynamics (dynamics excluding physics forcing tendency)

$$\partial\widehat{E}^{(\mathrm{2D})}_{\mathrm{dyn}} = \frac{\widehat{E}_{\mathrm{dAD}} - \widehat{E}_{\mathrm{dBD}}}{\Delta t_{\mathrm{dyn}}}, \tag{15}$$

where over a single dynamics substep $\Delta t_{\mathrm{dyn}} = \frac{\Delta t_{\mathrm{phys}}}{\texttt{nsplit}\times\texttt{rsplit}}$ (the loop bounds `nsplit`, `rsplit`, etc. are explained in Figure 1).

In CAM-SE the viscosity is explicit so one can compute the TE tendency due to hyperviscosity and its associated frictional heating

$$\partial\widehat{E}^{(\mathrm{hvis})}_{\mathrm{dyn}} = \frac{\widehat{E}_{\mathrm{dAH}} - \widehat{E}_{\mathrm{dBH}}}{\Delta t_{\mathrm{hvis}}}, \tag{16}$$

which, in CAM-SE, includes a frictional heating term from viscosity on momentum

$$\partial\widehat{E}^{(\mathrm{fheat})}_{\mathrm{dyn}} = \frac{\widehat{E}_{\mathrm{dAH}} - \widehat{E}_{\mathrm{dCH}}}{\Delta t_{\mathrm{hvis}}}, \tag{17}$$

where $\Delta t_{\mathrm{hvis}} = \frac{\Delta t_{\mathrm{phys}}}{\texttt{nsplit}\times\texttt{rsplit}\times\textit{hypervis\_subcycle}}$ is the time step of the substepped viscosity. Since the viscosity on momentum is compensated for via heating (frictional heating) $\partial\widehat{E}^{(\mathrm{hvis})}_{\mathrm{dyn}}$ "only" has contributions from viscosity on temperature and pressure-level thickness. In terms of TE conservation it would be beneficial if hyperviscosity on temperature and mass could be avoided. However, the hyperviscosity on mass and temperature is necessary to keep this model stable.

The residual

$$\partial\widehat{E}^{(\mathrm{res})}_{\mathrm{dyn}} = \partial\widehat{E}^{(\mathrm{2D})}_{\mathrm{dyn}} - \partial\widehat{E}^{(\mathrm{hvis})}_{\mathrm{dyn}}, \tag{18}$$

is the energy error due to inviscid dynamics and time-truncation errors.

The energy tendency due to vertical remapping is

$$\partial\widehat{E}^{(\mathrm{remap})}_{dyn} = \frac{\widehat{E}_{\mathrm{dAR}} - \widehat{E}_{\mathrm{dAD}}}{\Delta t_{\mathrm{remap}}}, \tag{19}$$

where $\Delta t_{\mathrm{remap}} = \frac{\Delta t_{\mathrm{phys}}}{\texttt{nsplit}}$.

The 3-D adiabatic dynamical core (no physics forcing but including friction) energy tendency is denoted

$$\partial\widehat{E}^{(\mathrm{adiab})}_{\mathrm{dyn}} = \partial\widehat{E}^{(\mathrm{2D})}_{\mathrm{dyn}} + \partial\widehat{E}^{(\mathrm{remap})}_{\mathrm{dyn}}. \tag{20}$$

5. $\partial\widehat{E}^{(\mathrm{pdc})}$: Total spurious energy tendency due to PDC errors is the difference between the energy tendency from physics and the energy tendency in the dynamics resulting from adding the physics increment to the dynamical core state

$$\partial\widehat{E}^{(\mathrm{pdc})} = \partial\widehat{E}^{(\mathrm{phys})}_{\mathrm{phys}} - \partial\widehat{E}^{(\mathrm{phys})}_{\mathrm{dyn}} \text{assuming } \partial\widehat{E}^{(\mathrm{discr})} = 0, \tag{21}$$

where

$$\partial\widehat{E}^{(\mathrm{phys})}_{\mathrm{dyn}} = \frac{\widehat{E}_{\mathrm{dBD}} - \widehat{E}_{\mathrm{dAF}}}{\Delta t_{\mathrm{pdc}}}, \tag{22}$$

and Δt_{pdc} is the time step between physics increments being added to the dynamical core. Remember we are dealing with average rates so terms computed with different time steps can be compared, but differences cannot be taken between terms sampled with different time steps.

The PDC TE tendency $\partial\widehat{E}^{(\mathrm{pdc})}$ makes use of TE formulas in dynamics and in physics so (21) is only well defined if the TE formula discrepancy is zero, $\partial\widehat{E}^{(\mathrm{discr})} = 0$. As mentioned in section 2.1, CAM-SE has the option to switch the continuous equations of motion conserving the TE used by CAM physics (8) instead of the more comprehensive TE formula (7).

In CAM-SE there are three PDC algorithms described in detail in section 3.6 in Lauritzen et al. (2018) and reviewed in section 1 here. One is state-update in which the entire physics increments are added to the dynamics state at the beginning of dynamics (referred to as `ftype=1`), in which case $\Delta t_{\mathrm{pdc}} = \Delta t_{\mathrm{phys}}$. Another is *dribbling* in which the physics tendency is split into `nsplit` equal chunks and added throughout dynamics (more precisely after every vertical remapping; referred to as `ftype=0` resulting in $\Delta t_{\mathrm{pdc}} = \frac{1}{\mathtt{nsplit}}\Delta t_{\mathrm{phys}}$), and then a *combination* of the two (referred to as `ftype=2`) where tracers (mass variables) use *state-update* (`ftype=1`) and all other physics tendencies use *dribbling* (`ftype=0`).

6. $\partial\widehat{E}^{(\mathrm{efix})}$: Global energy fixer tendency, defined in (14), is applied at the beginning of the parameterizations. The correction needed is the global average difference between the state passed from the dynamics and the state that was saved after the physics updated the state but before the dry mass correction. It includes all spurious sources from the dry mass correction, remappings between physics and dynamics, dynamical core, differing energy definitions (if present), hyperviscosity, and vertical remapping.

2.5. A Few Observations Regarding the Energy Budget Terms

It is useful to note that the energy fixer "fixes" energy errors for the dynamical core, pressure work error, PDC, and TE discrepancy

$$-\partial\widehat{E}^{(\mathrm{efix})}_{\mathrm{phys}} = \partial\widehat{E}^{(\mathrm{pwork})}_{\mathrm{phys}} + \partial\widehat{E}^{(\mathrm{adiab})}_{\mathrm{dyn}} + \partial\widehat{E}^{(\mathrm{pdc})} + \partial\widehat{E}^{(\mathrm{discr})}. \tag{23}$$

The forcing from the parameterizations, $\partial\widehat{E}^{(\mathrm{param})}_{\mathrm{phys}}$, does not appear in this budget (although the dynamical core state does "feel" the parameterization forcing) as the energy cycle for the parameterizations is, by design in CAM, closed (balanced by fluxes in/out of the physics columns). If $\partial\widehat{E}^{(\mathrm{discr})} = 0$, one can use (23) to diagnose energy dissipation in the dynamical core and PDC from quantities computed only in physics

$$\partial\widehat{E}^{(\mathrm{adiab})}_{\mathrm{dyn}} + \partial\widehat{E}^{(\mathrm{pdc})} = -\partial\widehat{E}^{(\mathrm{efix})}_{\mathrm{phys}} - \partial\widehat{E}^{(\mathrm{pwork})}_{\mathrm{phys}} \text{ for } \partial\widehat{E}^{(\mathrm{discr})} = 0. \tag{24}$$

This is useful if the diagnostics are not implemented in the dynamical core; in particular, if the *state-update* (`ftype=1`) PDC method is used then $\partial\widehat{E}^{(\mathrm{pdc})} = 0$ and the TE errors in the dynamical core can be computed without diagnostics implemented in the dynamical core. Also, (24) provides an alternative formula for $\partial\widehat{E}^{(\mathrm{pdc})}$ compared to (21):

$$\partial\widehat{E}^{(\mathrm{pdc})} = -\partial\widehat{E}^{(\mathrm{efix})}_{\mathrm{phys}} - \partial\widehat{E}^{(\mathrm{pwork})}_{\mathrm{phys}} - \partial\widehat{E}^{(\mathrm{adiab})}_{\mathrm{dyn}}, \text{ assuming } \partial\widehat{E}^{(\mathrm{discr})} = 0. \tag{25}$$

If $\partial\widehat{E}^{(\mathrm{pdc})} = 0$ (23) can be used to compute $\partial\widehat{E}^{(\mathrm{discr})}$

$$\partial\widehat{E}^{(\mathrm{discr})} = -\partial\widehat{E}^{(\mathrm{efix})}_{\mathrm{phys}} - \partial\widehat{E}^{(\mathrm{pwork})}_{\mathrm{phys}} - \partial\widehat{E}^{(\mathrm{adiab})}_{\mathrm{dyn}}, \text{ assuming } \partial\widehat{E}^{(\mathrm{pdc})} = 0. \tag{26}$$

Note that we cannot use (21) to compute $\partial\widehat{E}^{(\mathrm{discr})}$ since $\widehat{E}_{\mathrm{phys}} \neq \widehat{E}_{\mathrm{dyn}}$.

Table 1
TE Tendencies in Units of W/m^2 Associated With Various Aspects of CAM-SE Run in AMIP-Type Setup (Unless Otherwise Noted)

Descriptor	$\mathcal{N}$	`lcp_moist`	`ftype`	$\partial\widehat{E}^{(\text{pwork})}_{\text{phys}}$	$\partial\widehat{E}^{(\text{efix})}_{\text{phys}}$	$\partial\widehat{E}^{(\text{discr})}_{\text{phys}}$	$\partial\widehat{E}^{(\text{2D})}_{\text{dyn}}$	$\partial\widehat{E}^{(\text{hvis})}_{\text{dyn}}$	$\partial\widehat{E}^{(\text{fheat})}_{\text{dyn}}$	$\partial\widehat{E}^{(\text{res})}_{\text{dyn}}$	$\partial\widehat{E}^{(\text{remap})}_{\text{dyn}}$	$\partial\widehat{E}^{(\text{adiab})}_{\text{dyn}}$	$\partial\widehat{E}^{(\text{pdc})}$
TE consistent	1	false	1	0.312	0.300	0	−0.601	−0.608	0.565	0.007	−0.011	−0.613	0
"dribbling" A	1	false	0	0.315	0.313	0	−0.577	−0.584	0.568	0.007	−0.011	−0.588	**0.469**
"dribbling" B	1	false	2	0.316	0.341	0	−0.598	−0.606	0.563	0.008	−0.011	−0.609	**0.484**
vert limiter	1	false	1	0.317	0.472	0	−0.590	−0.597	0.509	0.006	**−0.199**	−0.789	0
smooth topo	1	false	1	0.315	**−0.008**	0	**−0.295**	**−0.300**	0.493	0.005	−0.012	**−0.307**	0
energy discr	5	true	1	0.332	−0.313	**0.594**	−0.603	-0.612	0.575	0.009	−0.011	−0.614	—
default	5	true	2	0.316	−0.272	—	−0.578	−0.587	0.579	0.010	−0.012	−0.589	—
QPC6	1	false	1	0.305	−0.169	0	**−0.129**	**−0.131**	0.477	0.001	−0.007	**−0.136**	0
FHS94	1	false	2	0			**−0.025**	**−0.025**	0.122	0	0.005	**−0.020**	—
FV	1	false	1	0.304	0.670	0	not impl.	not impl.	not impl.	not impl.	not impl.	**−0.974**	0
CSLAM	1	false	1	0.312	0.239	0	−0.547	−0.557	0.620	0.010	−0.011	−0.558	**−0.070**
CSLAM default	5	true	2	0.320	−0.342	—	−0.524	−0.537	0.641	0.013	−0.011	−0.535	—

Note. Column 1 is the identifier for the model configuration. See the text for a brief summary of these descriptors. They are defined in more detail in the following sections where the section titles also include the "Descriptor" from Table 1 to make it easier for the reader to match table entries with discussion in the text. Column 2 is $\mathcal{N}$ = `qsize_condensate_loading` identifying how many water species are thermodynamically/inertially active in the dynamical core (see section 2.1 for details). Column 3, `lcp_moist`, indicates whether or not the heat capacity includes water variables or not, and column 4 shows PDC method `ftype`. The TE tendencies $\partial\widehat{E}$ in columns 5–14 are defined in section 2.4. If $\partial\widehat{E}$ is less than 10^{-5} W/m^2, it is set to zero in the table. Significant changes compared to the baseline (*TE consistent* configuration) discussed in the main text are in bold font. Entries marked with "—" refer to TE tendencies that can not be directly calculated with the current framework, "not impl" refers to energy diagnostics not implemented in FV dynamical core, and blank in *FHS94* refers to the fact that this setup is run without energy fixer (parameterization not consistent with energy fixer), and hence there are no energy fixer numbers.

3. Results

A series of simulations have been performed with CESM2.1 using CAM version 6 (CAM6) physics (https://doi.org/10.5065/D67H1H0V) on NCAR's Cheyenne cluster (Computational and Information Systems Laboratory, 2017). All simulations are at nominally ∼1° horizontal resolution (for CAM-SE that is 30 × 30 elements on each cubed-sphere face and for CAM-FV its 192 × 288 latitudes-longitudes) and using the standard 32 levels in the vertical. Unless otherwise noted all simulations are 13 months in duration and the last 12 months are used in the analysis. Total energy budgets are summarized in Table 1 and discussed below. The first column gives identifying "Descriptors" which are briefly summarized below and defined in more detail in the following sections. The section titles also include the "Descriptor" from Table 1 to make it easier for the reader to match table entries with discussion in the text. Important changes to TE errors are marked with bold font in Table 1.

Various configurations are used and referred to in terms of the *COMPSET* (Component Set) value used in CESM2.1. The *COMPSET F2000climo* configuration refers to "real-world" AMIP (Atmospheric Model Intercomparison Project) type simulations using perpetual year 2000 SST (sea surface temperature) boundary conditions. The first seven simulations in the table (those above the horizontal line) are such AMIP-type simulations (F2000climo) with the first serving as a control for the six following variants. The remaining five simulation descriptors (below the horizontal line in Table 1) list their *COMPSET* or dynamical core settings.

The different configurations listed below (and discussed in separate subsections) are chosen to assess TE errors associated with different aspects of the dynamical core numerical algorithm, PDC method, surface conditions, etc. (as pointed out in parenthesis at the end of each item listing):

- *TE consistent*: The TE consistent version uses *state-update* PDC (`ftype=1`) described in section 3.1 (this configuration does not have PDC errors and it has the same TE definition in physics and dynamics; and hence the energetically most consistent setup in terms of least number of TE error terms);
- *dribbling A*: as *TE consistent* but with *dribbling* PDC (`ftype=0`) (section 3.2; this setup is used to assess PDC errors);
- *dribbling B*: as *TE consistent* but with *dribbling* combination PDC (`ftype=2`) (section 3.2; this setup is used to assess PDC errors);

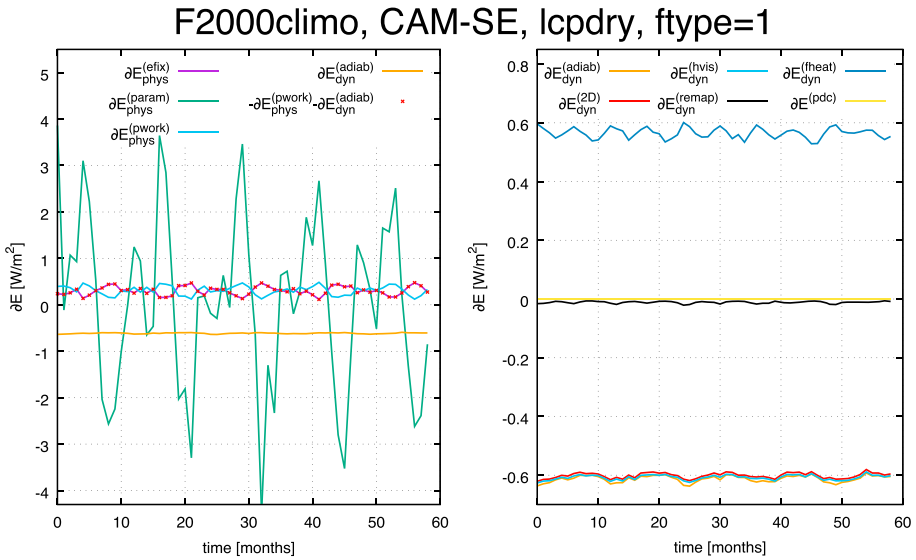

Figure 2. Monthly averaged total energy (TE) tendencies as a function of time for various aspects of the TE consistent configuration of CAM-SE run in AMIP-type configuration with perpetual year 2000 SSTs. Left figure shows $\partial\widehat{E}$ TE tendencies in physics and, for comparison, TE tendency for the adiabatic dynamical core. The right plot shows the breakdown of $\partial\widehat{E}$ for the dynamical core. These plots show that the energy tendency from the dynamical core is quite constant (to within ~0.02 W/m^2 or less), so only 1-month simulation is adequate to assess energy diagnostics for the dynamical core. For more details see section 3.1. CAM = Community Atmosphere Model; SE = spectral element; AMIP = Atmospheric Model Intercomparison Project.

- *vert limiter*: as *TE consistent* but using limiters in the vertical remapping of momentum (section 3.3; experiment is used to assess TE errors associated with shape-preserving limiters in vertical remapping);
- *smooth topo*: as *TE consistent* but using smoother topography (see section 3.4; experiment is used to assess TE sensitivity to surface roughness);
- *energy discr*: The version with energy discrepancy (but no PDC errors) described in section 3.5 (experiment is used to estimate energy discrepancy errors);
- *default*: as *energy discr* version but with `ftype=2` which is the current default CAM-SE (section 3.5; we assess this configuration since it is the default CAM-SE configuration);
- *QPC6*: A simplified aqua-planet setup based on the *TE consistent*, that is, an aqua-planet setup using CAM6 physics; an ocean covered planet in perpetual equinox, with fixed, zonally symmetric SSTs (Medeiros et al., 2016; Neale & Hoskins, 2000; section 3.6; experiment is used to assess TE errors in a simplified moist environment);
- *FSH94*: Dry dynamical core configuration based on Held-Suarez forcing which relaxes temperature to a zonally symmetric equilibrium temperature profile and simple linear drag at the lower boundary (Held & Suarez, 1994; section 3.7; experiment is used to assess if TE errors in one of the simplest climate test cases is representative of full model TE errors);
- *FV*: A configuration with the SE dynamical core replaced with the finite-volume core (section 3.8; experiment is used to assess TE errors of a different dynamical core);
- *CSLAM*: The quasi equal-area physics grid configuration of CAM-SE based on the TE consistent setup (section 3.9; used to assess TE errors associated with separating the dynamics grid from the physics grid); and
- *CSLAM default*: Same as *CSLAM* configuration but with `ftype=2` and all forms of water thermodynamically/inertially active in the dynamical core (setup is evaluated since it is the default CAM-SE-CSLAM setup).

3.1. *TE Consistent*: State-Update PDC (`ftype=1`) and No TE Formula Discrepancy

This configuration is the most energetically consistent in that the physical parameterizations and the continuous equations of motion on which the dynamical core is based, conserve the same TE (defined in equation (8)); and there are no spurious sources/sinks in PDC. Energetic consistency in dynamics and physics is obtained by setting $c_p^{(\ell)} \equiv c_p^{(d)}$ and $\mathcal{L}_{\text{all}} = \{\text{`}d\text{`}, \text{`}wv\text{`}\}$ in the dynamical core equations of motion and

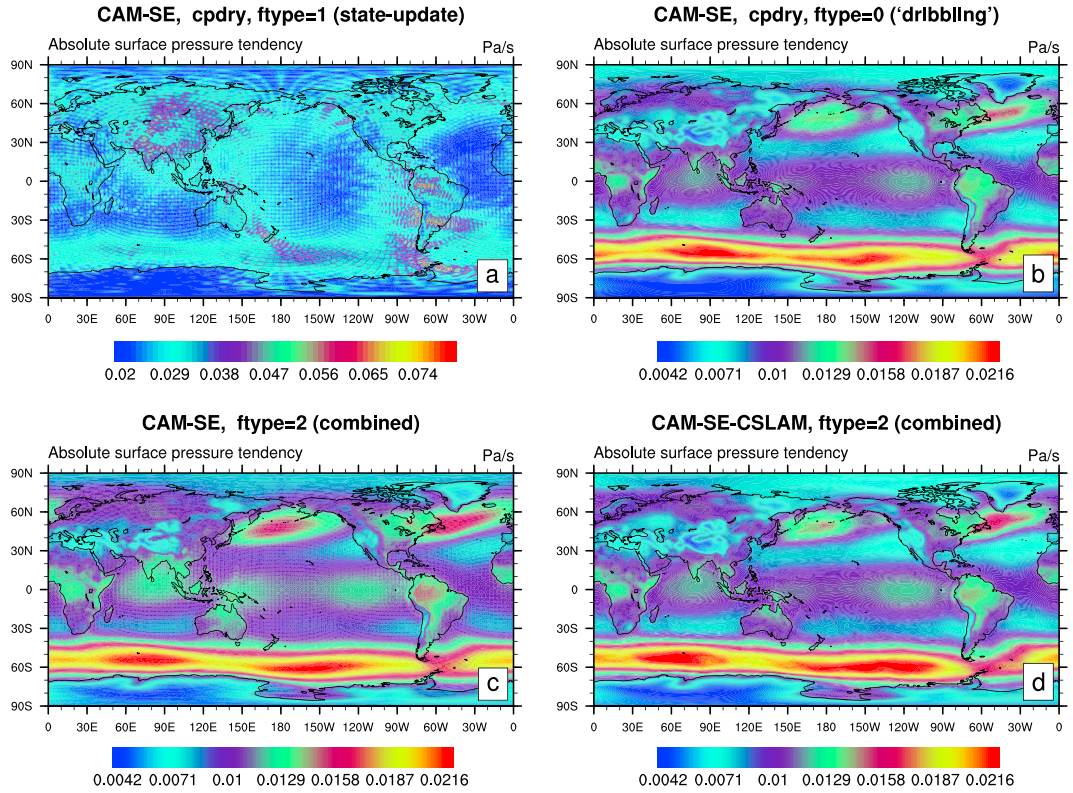

Figure 3. One-year average of the absolute surface pressure tendency for (a) the TE consistent configuration, (b) "dribbling" physics-dynamics coupling (PDC), (c) `ftype=2` PDC, and (d) CSLAM version of CAM-SE, respectively. Panel (a) has a closed PDC budget but spurious noise, (b) has no spurious noise but the mass budget in PDC is not closed (see Figure 6), (c) has a closed mass budget in PDC but some spurious noise at element boundaries, which is eliminated when using CAM-SE-CSLAM (d). Note, the smallest value in panel (a) is the largest in panels (b)–(d). CSLAM = Conservative Semi-LAgrangian Multi-tracer; CAM = Community Atmosphere Model; SE = spectral element.

TE computations. Associated namelist changes resulting in this configuration are `lcp_moist=.false.`, `se_qsize_condensate_loading=1`, and `ftype=1`. We use this configuration as a baseline since it has the least number of TE error terms ($\partial\widehat{E}^{(\mathrm{pdc})} = \partial\widehat{E}^{(\mathrm{discr})} = 0$).

The TE consistent configuration in AMIP-type simulation (*F2000climo*) is used to compute baseline TE tendencies, which will be used to compare with other model configurations. First, we establish how long an average is needed to get robust TE tendency estimates. Figure 2 shows $\partial\widehat{E}$ for various aspects of CAM-SE as a function of time. The simulation length is 5 years and monthly average values are used for the analysis. First, consider the left plot. The TE tendency from parameterizations ($\partial\widehat{E}^{(\mathrm{param})}_{\mathrm{phys}}$) show significant variability with an amplitude of approximately 2.5 W/m^2. As noted above this term does not figure in the spurious TE budget. The net source/sink provides an equal and opposite term to balance it. That said, the variability is reflected onto the TE tendency due to pressure work error $\partial\widehat{E}^{(\mathrm{pwork})}_{\mathrm{phys}} \approx 0.32 \pm 0.08$ W/m^2. On the scale used in the left-hand plot the TE tendency of the adiabatic dynamical core $\partial\widehat{E}^{(\mathrm{adiab})}_{\mathrm{dyn}}$ does not seem to be affected by $\partial\widehat{E}^{(\mathrm{param})}_{\mathrm{phys}}$ or $\partial\widehat{E}^{(\mathrm{pwork})}_{\mathrm{phys}}$ in terms of variability, and remains stable at approximately -0.6 ± 0.02 W/m^2. The TE fixer, in this model configuration, fixes $\partial\widehat{E}^{(\mathrm{adiab})}_{\mathrm{dyn}}$ and $\partial\widehat{E}^{(\mathrm{pwork})}_{\mathrm{phys}}$. Since the TE imbalance in the adiabatic dynamics remains approximately constant and the TE tendency associated with pressure work error has variability, the TE tendency from the $\partial\widehat{E}^{(\mathrm{efix})}_{\mathrm{phys}}$ has variability; $\partial\widehat{E}^{(\mathrm{efix})}_{\mathrm{phys}} \approx 0.30 \pm 0.08$ W/m^2. As a consistency check $-\partial\widehat{E}^{(\mathrm{adiab})}_{\mathrm{dyn}} - \partial\widehat{E}^{(\mathrm{pwork})}_{\mathrm{phys}}$ is plotted with asterisk's and they coincide (as expected) with $\partial\widehat{E}^{(\mathrm{efix})}_{\mathrm{phys}}$ fulfilling (23).

The right-hand plot in Figure 2 shows a breakdown of the dynamical core TE tendencies. The majority of the TE errors are due to hyperviscosity on temperature and pressure, $\partial\widehat{E}^{(\mathrm{hvis})}_{\mathrm{dyn}} \approx -0.61 \pm 0.01$ W/m^2. The diffusion

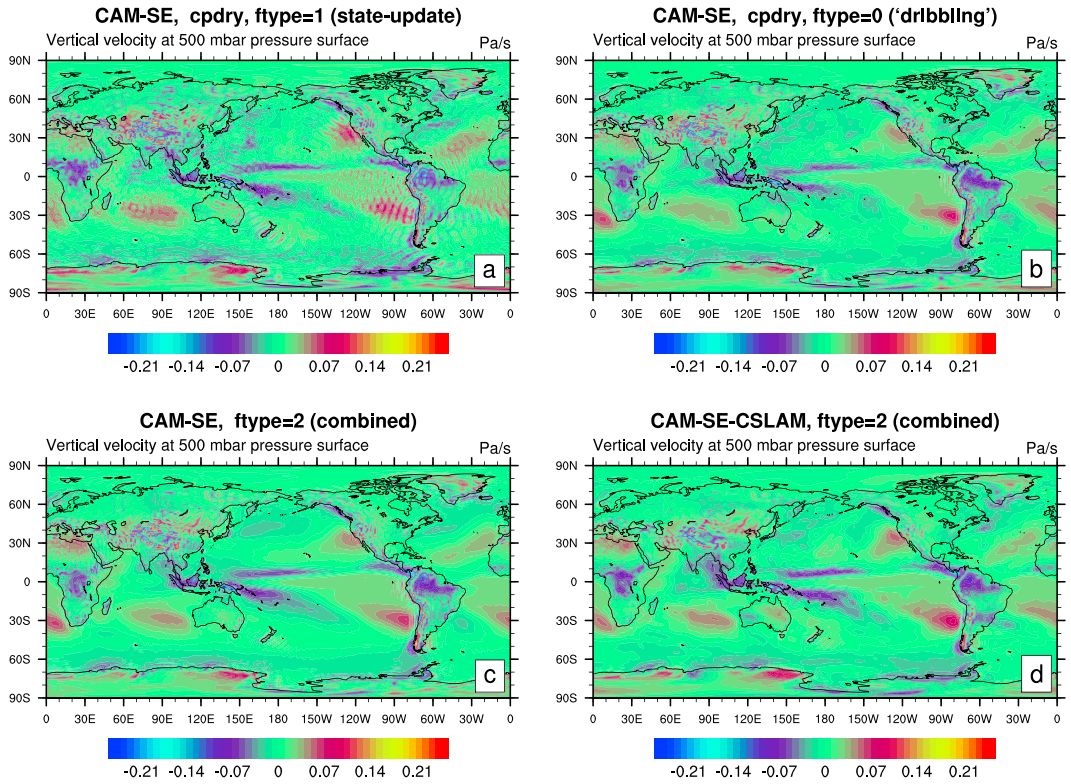

Figure 4. Same as Figure 3 but for 500-hPa vertical pressure velocity. Note the ringing patterns off the West Coast of South America and around the Himalayas in CAM-SE (a–c) that are eliminated with CAM-SE-CSLAM (d) that makes use of a quasi equal-area physics grid. CAM = Community Atmosphere Model; SE = spectral element; CSLAM = Conservative Semi-LAgrangian Multi-tracer.

of momentum is added back as frictional heating and is therefore not part of $\partial\widehat{E}^{(\mathrm{hvis})}_{\mathrm{dyn}}$. The frictional heating is a significant term in the TE tendency budget $\partial\widehat{E}^{(\mathrm{fheat})}_{\mathrm{dyn}} \approx 0.56 \pm 0.02$ W/m^2 and exhibits some variability but with a rather small amplitude. The remaining TE error in the floating Lagrangian dynamics is inviscid dissipation and time truncation errors $\partial\widehat{E}^{(\mathrm{res})}_{\mathrm{dyn}} = \partial\widehat{E}^{(\mathrm{2D})}_{\mathrm{dyn}} - \partial\widehat{E}^{(\mathrm{hvis})}_{\mathrm{dyn}} \approx 0.007$ W/m^2. The TE tendency from vertical remapping is approximately $\partial\widehat{E}^{(\mathrm{remap})}_{\mathrm{dyn}} \approx -0.01$ W/m^2. To within $\sim$0.02 W/m^2 the dynamical core TE tendency terms can be computed from just 1 month average TE integrals. The TE tendencies computed in physics, excluding $\partial\widehat{E}^{(\mathrm{param})}_{\mathrm{phys}}$, exhibit more variability and are only accurate to $\sim$0.1 W/m^2 after a 1-month average.

While it is advantageous to use state-update PDC algorithm (`ftype=1`) in terms of having no spurious TE tendency from coupling, $\partial\widehat{E}^{(\mathrm{pdc})} = 0$, it does result in spurious gravity waves in the simulations (see, e.g., Figure 5 in Gross et al., 2018). Figure 3a shows a 1-year average of $|\frac{\mathrm{d}p_s}{\mathrm{d}t}|$, a measure of high-frequency gravity wave noise. It clearly exhibits unphysical oscillations coinciding with element boundaries. Details of the spectral-element method, its coupling to physics, and associated noise issues are discussed in detail in Herrington et al. (2019). The noise in the solutions is even visible in the 500-hPa pressure velocity annual average (Figure 4a). This issue can be alleviated by using a shorter physics time step so that the physics increments are smaller (not shown). Climate modelers have historically not pursued a shorter physics time step in production configurations as climate parameterizations are computationally expensive and there is a large sensitivity to physics time steps in the simulated climate (e.g., Wan et al., 2015; Williamson & Olson, 2003).

3.2. *"Dribbling" A/B*: Non-TE Conservative PDC (`ftype=0,2`)

Before discussing the impact of different PDC methods on the TE budget, we discuss element boundary noise issues in CAM-SE which are related to PDC method. This motivates the different PDC methods implemented in CAM-SE.

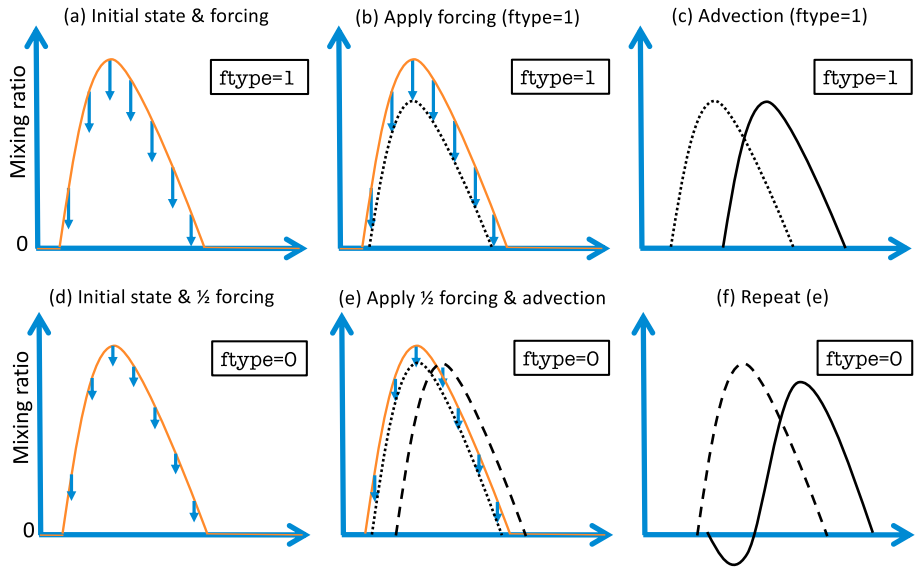

Figure 5. A schematic of *state-update* (`ftype=1`; a–c) and "dribbling" (`ftype=0`; d–f) physics-dynamics coupling algorithms. See section 3.2 for details.

3.2.1. Spurious Element Boundary Noise From PDC

When switching to *dribbling* PDC algorithm (`ftype=0`) in which the tendencies from physics are added throughout the dynamics (in this case twice per physics time step), then the noise issues described in previous section disappear (Figures 3b and 4b). That said, there is a significant issue with this approach; the tracer mass budgets may not be closed. How this comes about is illustrated in Figure 5 and explained in the next paragraph.

The orange curve on Figures 5a, 5b, 5d, and 5e is the initial state of, for example, cloud liquid mixing ratio as a function of location, for example, longitude. Cloud liquid is zero outside of clouds and hence provides a good example for the purpose of this illustration. The light blue arrows show the increments (in terms of length of arrow) computed by the parameterizations based on the initial state and scaled for the partial update with *dribbling* (`ftype=0`). With *state-update* (`ftype=1`) the increments from physics are added to the dynamical core state (dotted line on Figure 5b) before the dynamical core advances the solution in time. The parameterizations are designed to not drive the mixing ratios negative so the state-update in dynamics will not generate negatives (or overshoots). Then the dynamical core advects the distribution (solid curve on Figure 5c). With *dribbling* (`ftype=0`) the physics increments are split into equal chunks (in this illustration two; blue arrows on Figure 5d). Half of the physics increments are added to the initial state (dotted line on Figure 5e), and then dynamics advects the distribution half of the total dynamical core steps (dashed line on Figure 5e). Then the other half of the physics increments are applied (in the same location as they were computed by physics). Now after the previous/first advection step the cloud liquid distribution has moved and the mixing ratio may be zero (or less than the increment prescribed by physics), where the physics forcing is applied (e.g., left side of dashed curve). Hence, the physics increment is driving the mixing ratios negative in those locations. Thereafter, the distribution is advected (solid curve on Figure 5f). In CAM the increments added in the dynamical core are limited so that they drive the mixing to zero (but not negative) if this problem occurs. This leads to a net source of mass compared to the mass change that the parameterizations prescribe (see Figure 6). Although the average source of mass is small each time step, it always has the same sign (i.e., it is a bias) and therefore accumulates. Zhang et al. (2018) estimated that this spurious source of mass is equivalent to ~10-cm sea-level rise per decade in coupled climate simulation experiments.

The majority of the noise with *state-update* (`ftype=1`) PDC method comes from momentum sources/sinks and heating/cooling. A way to alleviate noise problems and, at the same time, close the tracer mass budgets (in PDC) is to use *state-update* (`ftype=1`) coupling for tracers and *dribbling* (`ftype=0`) coupling for momentum and temperature (referred to as *combination*, `ftype=2`). Figure 3c shows the noise diagnostic $|\frac{dp_s}{dt}|$ for *combination* (`ftype=2`) coupling. Figure 3c looks very similar to Figure 3b but there is some noise near element boundaries. That said, in terms of vertical pressure velocities *combination* (`ftype=2`)

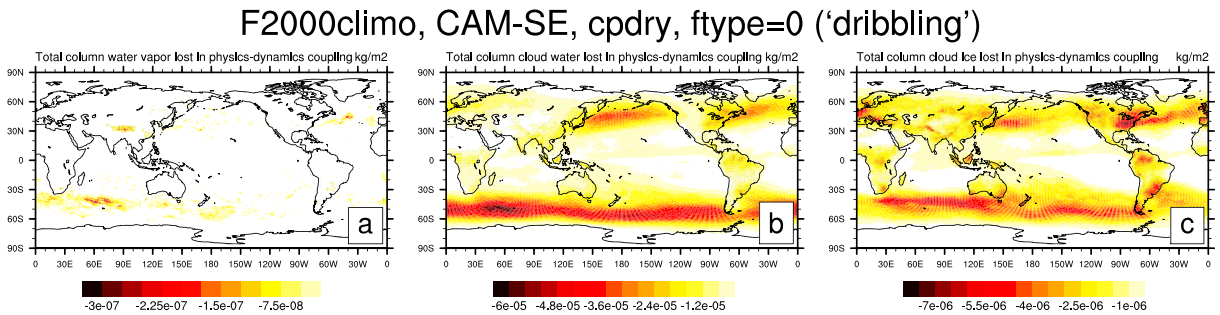

Figure 6. One-year average of mass (kg/m^2) "clipped" in physics-dynamics coupling (so that state is not driven negative) when using `ftype=0` ('dribbling') physics-dynamics coupling for (a) water vapor, (b) cloud liquid, and (c) cloud ice, respectively. Interestingly, the element boundaries systematically show in the plots which is likely related to the anisotropy of the quadrature grid (Herrington et al., 2019).

and *dribbling* (`ftype=0`) climates are similar in terms of the level of noise (Figures 4b and 4c). The element noise in CAM-SE with *combination* (`ftype=2`) seen in both $|\frac{dp_s}{dt}|$ and 500-hPa pressure velocity can be "removed" by using CAM-SE-CSLAM (Figure 3d), which uses a quasi equal-area physics grid and CSLAM (Lauritzen et al., 2010) consistently coupled to the SE method (Lauritzen et al., 2017). The noise patterns in vertical velocity off the western coast of South America are present in all CAM-SE simulations (and hence not related to PDC algorithm) are also removed by using CAM-SE-CSLAM (Herrington et al., 2019).

3.2.2. Spurious TE Tendencies From PDC

When using the same TE formula in the dynamical core and physics the spurious TE tendency from PDC can be assessed. As described in item 5 (section 2.3), PDC errors can be attributed to underlying pressure changes during the dribbling of temperature and velocity component increments as well as PDC clipping errors in the water variables (the process in which clipping occurs is described in detail in the previous subsection). The TE error associated with clipping PDC error occurs when the mass change prescribed by physics that is consistent with the fluxes in/out of the physics column does not equal the actual mass change applied to the dynamical core state due to clipping.

For `ftype=2` PDC only the increment for temperature and momentum are *dribbled*, whereas tracer mass is state-updated (no clipping errors). This results in a spurious PDC TE tendency of $\partial\widehat{E}^{(\mathrm{pdc})} = -0.484$ W/m^2. When using `ftype=0` PDC also tracer increments are *dribbled* (hence there are clipping PDC errors) a similar TE tendency results $\partial\widehat{E}^{(\mathrm{pdc})} = -0.469$ W/m^2. The difference between the TE PDC tenendency for `ftype=2` and `ftype=0` provides an estimate of the TE PDC clipping error. The clipping PDC TE tenendency is very small 0.015 W/m^2.

3.3. *Vert limiter*: Limiters on Vertical Remapping of Momentum

CAM-SE uses a floating Lagrangian vertical coordinate (Lin, 2004; Starr, 1945) which requires the remapping of the atmospheric state from floating levels back to reference levels to maintain computational stability and to provide state data consistent with the physics formulation. The mapping algorithm is based on the mass conservative PPM (Piecewise Parabolic Method) with options for shape-preserving limiters. In CAM-SE momentum components and internal energy are used as the variables mapped in the vertical (Lauritzen et al., 2018) and, contrary to earlier versions of CAM-SE, there is no limiter on the remapping of wind components. If the shape-preserving limiter is used for momentum mapping then the TE dissipation increases by over an order of magnitude from ∼0.01 W/m^2 to ∼0.2 W/m^2 (Table 1).

3.4. *Smooth topo*: Smoother Topography

Topography for CAM is generated using a new version of the software/algorithm described in Lauritzen et al. (2015) that is available at this website (https://github.com/NCAR/Topo). The updates to the software includes smoothing algorithms and the computation of subgrid-scale orientation of topography.

The default topography in CAM-SE uses the same amount of topography smoothing as CAM-FV (distance weighted smoother applied to the raw topography on ∼3 km cubed-sphere grid with a smoothing radius of 180 km referred to as *C*60). When the topography is smoother (in this case using *C*92 smoothing, i.e., smoothing radius of approximately 276 km) the hyperviscosity operators are less active leading to reduced TE errors, that is, $\partial\widehat{E}^{(\mathrm{hvis})}_{\mathrm{dyn}}$ is reduced in half from approximately −0.6 W/m^2 to −0.3 W/m^2. The vertical remapping TE error, however, remains approximately the same. Since the pressure work error is approximately 0.3 W/m^2

it almost exactly compensates for the TE tendency from the dynamical core $\partial\widehat{E}^{(\text{adiab})}_{\text{dyn}}$. Hence, if one would only diagnose the TE tendency from the energy fixer one could mistakenly conclude that the model universally conserves TE when, in fact, there are compensating TE errors in the system. These compensating errors can only be diagnosed through a careful breakdown of the total TE tendencies.

3.5. *Default*: TE Formula Discrepancy Errors

To assess the TE errors due to the discrepancy in the energy formula used by dynamics and physics, a simulation using *state-updating* (`ftype=1`, no *'dribbling'* errors) and thermodynamically/inertially active condensates in the dynamical core (*qsize_condensate_loading* $= 5$) and consistent/accurate associated heat capacities $c_p^{(\ell)}$ (namelist `lcp_moist=.true.`) has been performed. In this setup the continuous equations of motion in the dynamical core conserve an energy different from physics, and the energy fixer will restore the "physics" version of energy. Despite the dynamical core now using a more comprehensive formula for energy, the TE dissipation terms in the dynamical core are roughly the same as in the energy consistent versions of the model. Using (26) we can assess the TE energy discrepancy errors which result in ~0.59 W/m^2. Taylor (2011) found a similar result just from using the more comprehensive formula for heat capacity (based on dry air and water vapor) and not including thermodynamically/inertially active condensates. As noted before this formulation inconsistency is due to the evolutionary nature of CAM development and it is the intention to remove this inconsistency in future versions of the model.

The default version of CAM-SE uses this configuration but with *combination* (`ftype=2`), which has similar TE characteristics (see Table 1). That said, the PDC error from *dribbling* momentum and temperature tendencies and the energy discrepancy errors can not be separated in this configuration:

$$\partial\widehat{E}^{(\text{pdc})} + \partial\widehat{E}^{(\text{discr})} = 0.546\,\text{W/m}^2, \tag{27}$$

using (23). With *state-updating* (`ftype=1`) (i.e., $\partial\widehat{E}^{(\text{pdc})} = 0$) the energy discrepancy error was 0.594 W/m^2 and in the energy consistent setup (i.e., $\partial\widehat{E}^{(\text{discr})} = 0$) but using *dribbling* (`ftype=2`) we got $\partial\widehat{E}^{(\text{pdc})} = 0.484$ W/m^2. So if the PDC errors and energy discrepancy errors in the different configurations would be additive, one would have expected $\partial\widehat{E}^{(\text{pdc})} + \partial\widehat{E}^{(\text{discr})}$ to be over 1 W/m^2, which is clearly not the case (27). Again, it must be concluded that there are canceling errors in the system.

3.5.1. Two-Dimensional Structure of TE Errors

Figure 7 shows the two-dimensional spatial structure of column-integrated TE tendencies for for the *default* configuration. The first plot (Figure 7a) shows column integrated $\partial E^{(\text{param})}$, that is, the spatial structure of the "physical" TE tendency. Only contours from $\pm$150 W/m^2 are shown although the actual range (noted above color bar) is -148.3 W/m^2 to 1,770 W/m^2. The larger positive values occur only at a small number of grid points (e.g., mountains of New Guinea). The column-integrated dynamical core TE tendency $\partial\widehat{E}^{(\text{adiab})}$ (Figure 7c) approximately balances $\partial E^{(\text{param})}$; this is expected in an AMIP simulation that, if integrated long enough, should reach radiative equilibrium. The TE pressure work error tendency $\partial E^{(\text{pwork})}$ (Figure 7b) is, as expected, largest where precipitation and evaporation is largest. The last three plots show terms in the dynamical core budget: column-integrated TE tendency from the 2-D adiabatic dynamical core, $\partial\widehat{E}^{(\text{2D})}$, vertical remapping, $\partial\widehat{E}^{(\text{remap})}$, and frictional heating, $\partial\widehat{E}^{(fheat)}$. The adiabatic dynamical core TE tendency is dominated by the tendencies from the floating Lagrangian (quasi-horizonal) dynamics. The frictional heating TE tendency is largest over/near topography. Similarly for vertical remapping but, in addition, there are large TE tendencies in areas of large updrafts/downdrafts over ocean.

3.6. *QPC6*: Simplified Surface

By running the model in aqua-planet configuration one can assess the effect of simplifying the surface boundary condition. In particular, without topography forcing the dynamical core is not challenged with respect to stationary near-grid-scale forcing. The TE tendency with respect to pressure work error remains the same $\partial\widehat{E}^{(\text{pwork})}_{\text{phys}}$ as the AMIP-type simulations; however, the adiabatic dynamical core TE tendency reduces to $\partial\widehat{E}^{(\text{adiab})}_{\text{dyn}} = -0.14$ W/m^2 (approximately a factor 4 reduction). Most of that reduction is due to viscosity $\partial\widehat{E}^{(\text{hvis})}_{\text{dyn}} = -0.13$ W/m^2. The frictional heating is roughly the same as AMIP $\partial\widehat{E}^{(\text{fheat})}_{\text{dyn}} = 0.48$ W/m^2 as is the vertical remapping $\partial\widehat{E}^{(\text{remap})}_{\text{dyn}} = -0.01$ W/m^2. To evaluate the dynamical cores diffusion of TE it is therefore important to asses the model in a configuration with topography as the wave dynamics generated by topography leads to more active diffusion operators.

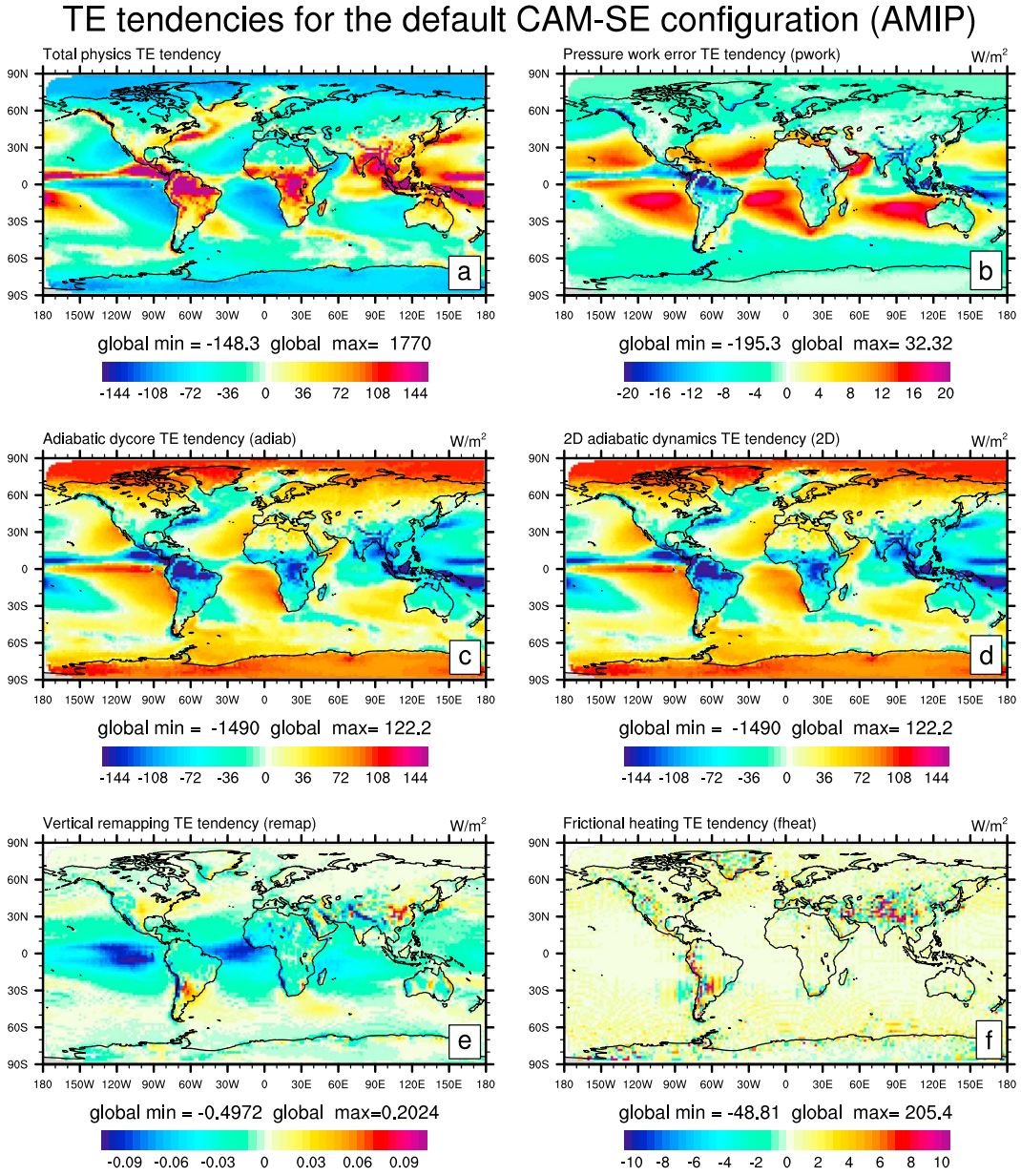

Figure 7. Two-dimensional spatial structure of column-integrated total energy (TE) tendencies for different terms in the TE tendency budget using the *default* configuration: Column-integrated (a) $\partial E^{(\text{param})}$, (b) $\partial E^{(\text{pwork})}$, (c) $\partial E^{(\text{adiab})}$, (d) $\partial E^{(\text{2D})}$, (e) $\partial E^{(\text{remap})}$, and (f) $\partial E^{(\text{fheat})}$. Above each color bar the global minimum and maximum TE tendencies are noted as there are small number of grid points where the TE tendencies are much larger than the color bar range. CAM = Community Atmosphere Model; SE = spectral element; AMIP = Atmospheric Model Intercomparison Project.

3.7. *FHS94*: Simplified Physics (No Moisture)

Simplifying the setup even further by replacing the parameterizations with relaxation toward a zonally symmetric temperature profile and simple boundary layer friction (Held-Suarez forcing) as well as excluding moisture, the TE errors in the dynamical core decreases even further to ~0.002 W/m^2, since there is no small scale forcing. Small scales are only created by the nonlinear dynamics and the physics works to damp them. Hyperviscosity is less active leading to significant reductions compared to aqua-planet and 'real-world' simulation results. The TE diffusion in vertical remapping reduces by an order of magnitude compared to the aqua-planet simulations (~0.0005 W/m^2). This further emphasizes that TE diffusion assessment in a simplified setup is not necessarily telling for the dynamical cores performance with moist physics and topography that challenge the dynamical core in terms of strong grid-scale forcing.

3.8. *FV*: Changing Dynamical Core to FV

As a comparison the TE error characteristics of the CAM-FV dynamical core are assessed. Although the TE diagnostics have not been implemented in the CAM-FV dynamical core, the TE diagnostics in CAM physics are independent of dynamical core and can therefore be activated with CAM-FV. The CAM-FV dynamical core uses state-update PDC (`ftype=1`) ($\partial\widehat{E}^{(\mathrm{pdc})} = 0$) and the same TE definition as CAM physics ($\partial\widehat{E}^{(\mathrm{discr})} = 0$). Hence (24) can be used to compute the TE errors of the CAM-FV dynamical core, $\partial\widehat{E}^{(\mathrm{adiab})}_{\mathrm{dyn}} \approx -1$ W/m^2. As we do not have the breakdown of $\partial\widehat{E}^{(\mathrm{adiab})}_{\mathrm{dyn}}$ it can not be determined how much of the TE errors are due to the vertical remapping. Furthermore, CAM-FV contains intrinsic dissipation operators (limiters in the flux operators) making it difficult to assess TE sources/sinks due to dissipation. Note that the pressure work error even with a change of dynamical core remains approximately the same as the CAM-SE configurations.

3.9. *CSLAM*: Quasi Equal-Area Physics Grid

This configuration was discussed in the context of element noise in section 3.2.1. By averaging the dynamics state of an equal-partitioning (in central angle cubed-sphere coordinates) of the elements, the element-boundary noise found in CAM-SE can be removed. Lauritzen et al. (2018) argue that this way of computing the state for the physics is more consistent with physics in terms of providing a cell-averaged state instead of irregularly spaced point (quadrature) values. In order to achieve a closed mass budget, this configuration uses CSLAM for tracer transport rather than SE transport. That said, the physics columns no longer coincide with the quadrature grid and there are TE errors associated with mapping state and tendencies between the two grids.

In this configuration the energy diagnostics computed in the dynamical core are computed on the quadrature grid and the energy diagnostics computed in physics are on the physics grid. If the TE consistent configuration is used (`ftype=1`, `qsize_condensate_loading=1`, `lcp_moist=.false.`) then the PDC errors, $\widehat{E}^{(\mathrm{pdc})}$, computed with (21) are entirely due to mapping state from quadrature grid to physics grid and mapping tendencies back the quadrature grid from the physics grid. The results is $\widehat{E}^{(\mathrm{pdc})} = -0.07$ W/m^2 which is a rather small error compared to other terms in the TE budget.

Due to similar noise problems with CAM-SE-CSLAM when using `ftype=1` that were observed in CAM-SE (Figures 3 and 4), the default version of CAM-SE-CSLAM uses `ftype=2`. Again, PDC errors and TE discrepancy errors cannot be separated; $\partial\widehat{E}^{(\mathrm{pdc})} + \partial\widehat{E}^{(\mathrm{discr})} = 0.557$ W/m^2.

4. Conclusions

A detailed TE error analysis of the CAM using version 6 physics (included in the CESM2.1 release) running at approximately 1° horizontal resolution has been presented. In the global climate model there can be many spurious contributions to the TE budget. These errors can be divided into four categories: physical parameterizations, adiabatic dynamical core, the coupling between physics and dynamics, and TE definition discrepancies between dynamics and physics. The latter is not by design but through the evolutionary nature of model development. By capturing the atmospheric state at various locations in the model algorithm, a detailed budget of TE errors can be constructed. The net spurious TE energy errors are compensated with a global energy fixer (providing a global uniform temperature increment) every physics time step.

In CAM physics the parameterizations have, by design, a closed energy budget (change in TE is balanced by fluxes in/out the top and bottom of physics columns) if it is assumed that pressure is not modified. However, the pressure changes due to fluxes of mass (e.g., water vapor) in/out of the column which changes energy (referred to as pressure work error). The pressure work error with the full moist physics configuration is very stable across different configurations at ∼0.3 W/m^2. The TE errors in the SE dynamical core varies across configurations. Aspects that influence TE is the presence of topography, the amount of topography smoothing and moist physics. By smoothing topography more the TE error is cut in half from ~ -0.6 W/m^2 to ~ -0.3 W/m^2; and reduces by a factor of 6 (~ -0.1 W/m^2) if no topography is present at all (aqua-planet configuration). Moist physics forcing also contributes significantly to the TE budget. For example, in the dry Held-Suarez setup TE dissipation of the SE dynamical core reduces to −0.03 W/m^2. Topography and moist physics force the dynamical core at the grid scale and hence the viscosity operators are more active. Consistent with this statement is that the changes in TE discussed so far are almost entirely due to the viscosity operator TE dissipation. For CAM-SE the spurious TE dissipation in the adiabatic dynamical core is $\sim -0.6 W/m^2$ in "real-world" configurations. For comparison, CAM-FV's spurious TE change due to the adiabatic dynamical core is ~ -1 W/m^2.

By further breaking down the TE dissipation in the SE dynamical core it is observed the vertical remapping accounts for only ~ -0.01 W/m^2. That said, if the shape-preserving limiters in the vertical remapping are invoked the TE dissipation increases 20-fold to ~ -0.2 W/m^2. In CAM-SE the kinetic energy dissipation is added as heating in the thermodynamic equation (also referred to as frictional heating). The frictional heating remains very stable across configurations that include moisture (~ 0.5 W/m^2) and reduces drastically for dry atmosphere setups (factor 4 reduction to (~ 0.12 W/m^2)). Hence, this term is an important term in the TE budget. The TE budget for the dynamical core is dominated by TE change due to hyperviscosity; TE errors due to time-truncation and frictionless equations of motion are negligible. Errors associated with PDC (if applicable) are approximately 0.5 W/m^2. Due to the evolutionary nature of model development the SE dynamical core's continuous equation of motion conserve a more comprehensive TE compared to the physical parameterizations. This TE discrepancy leads to an approximately 0.5 W/m^2 total energy source. Running physics on a different grid than the dynamical introduces TE mapping errors such as in CAM-SE-CSLAM. These errors are, however, rather small -0.07 W/m^2.

A purpose of this paper is to better understand the energy characteristics of CAM and to encourage modeling groups to perform similar analysis to better understand the total energy flow in the atmospheric component of Earth system models. As has been demonstrated in this paper there can easily be compensating errors in the system which can not be identified without a detailed TE analysis. The analysis in this paper only considers 1° horizontal resolution and 32 levels in the vertical. The TE numbers and clipping results may not be accurate for other choices of horizontal and vertical resolutions.

Acknowledgments
We thank one anonymous reviewer, Hui Wan, and Phil Rasch for their helpful comments that significantly improved the clarity of the manuscript. The National Center for Atmospheric Research is sponsored by the National Science Foundation. Computing resources (doi:10.5065/D6RX99HX) were provided by the Climate Simulation Laboratory at NCAR's Computational and Information Systems Laboratory, sponsored by the National Science Foundation and other agencie\uline{}s. The data used to perform the energy analysis can be found at this website (https://github.com/PeterHjortLauritzen/2018-JAMES-energy).

References

Boville, B. A. (2000). Toward a complete model of the climate system. In P. Mote & A. O'Neill (Eds.), *Numerical Modeling of the Global Atmosphere in the Climate System, Numerical Modeling of the Global Atmosphere in the Climate System* (pp. 419–442). Berlin: Springer Science & Business Media. https://doi.org/10.1007/978-3-642-11640-7_12

Computational and Information Systems Laboratory (2017). *Cheyenne: HPE/SGI ICE XA System (Climate Simulation Laboratory)*. Boulder, CO: National Center for Atmospheric Research. https://doi.org/10.5065/D6RX99HX

Eldred, C., & Randall, D. (2017). Total energy and potential enstrophy conserving schemes for the shallow water equations using Hamiltonian methods—Part 1: Derivation and properties. *Geoscientific Model Development*, *10*(2), 791–810. https://doi.org/10.5194/gmd-10-791-2017

Gross, M., Wan, H., Rasch, P. J., Caldwell, P. M., Williamson, D. L., Klocke, D., et al. (2018). Physics-dynamics coupling in weather, climate and earth system models: Challenges and recent progress. *Monthly Weather Review*, *146*, 3505–3544. https://doi.org/10.1175/MWR-D-17-0345.1

Held, I. M., & Suarez, M. J. (1994). A proposal for the intercomparison of the dynamical cores of atmospheric general circulation models. *Bulletin of the American Meteorological Society*, *75*, 1825–1830.

Herrington, A. R., Lauritzen, P. H., Taylor, M. A., Goldhaber, S., Eaton, B. E., Bacmeister, J. T., et al. (2019). Physics-Dynamics Coupling with Element-Based High-Order Galerkin Methods: Quasi Equal-Area Physics Grid. *Monthly Weather Review*, *147*, 69–84. https://doi.org/10.1175/MWR-D-18-0136.1

Jablonowski, C., & Williamson, D. L. (2011). The pros and cons of diffusion, filters and fixers in atmospheric general circulation models. In P. H. Lauritzen, R. D. Nair, C. Jablonowski, & M. Taylor (Eds.), *Numerical techniques for global atmospheric models* (Vol. 80, pp. 381–493), Lecture Notes in Computational Science and Engineering. Berlin: Springer. https://doi.org/10.1007/978-3-642-11640-7_13

Kasahara, A. (1974). Various vertical coordinate systems used for numerical weather prediction. *Monthly Weather Review*, *102*(7), 509–522.

Lauritzen, P. H., Bacmeister, J. T., Callaghan, P. F., & Taylor, M. A. (2015). NCAR_Topo (v1.0): NCAR global model topography generation software for unstructured grids. *Geoscientific Model Development*, *8*(12), 3975–3986. https://doi.org/10.5194/gmd-8-3975-2015

Lauritzen, P. H., Bacmeister, J. T., Dubos, T., Lebonnois, S., & Taylor, M. A. (2014). Held-Suarez simulations with the Community Atmosphere Model Spectral Element (CAM-SE) dynamical core: A global axial angular momentum analysis using Eulerian and floating Lagrangian vertical coordinates. *Journal of Advances in Modeling Earth Systems*, *6*, 129–140. https://doi.org/10.1002/2013MS000268

Lauritzen, P. H., Nair, R. D., Herrington, A. R., Callaghan, P., Goldhaber, S., Dennis, J. M., et al. (2018). NCAR release of CAM-SE in CESM2.0: A reformulation of the spectral-element dynamical core in dry-mass vertical coordinates with comprehensive treatment of condensates and energy. *Journal of Advances in Modeling Earth Systems*, *10*, 1537–1570. https://doi.org/10.1029/2017MS001257

Lauritzen, P. H., Nair, R. D., & Ullrich, P. A. (2010). A conservative semi-Lagrangian multi-tracer transport scheme (CSLAM) on the cubed-sphere grid. *Journal of Computational Physics*, *229*, 1401–1424. https://doi.org/10.1016/j.jcp.2009.10.036

Lauritzen, P. H., Taylor, M. A., Overfelt, J., Ullrich, P. A., Nair, R. D., Goldhaber, S., & Kelly, R. (2017). CAM-SE-CSLAM: Consistent coupling of a conservative semi-lagrangian finite-volume method with spectral element dynamics. *Monthly Weather Review*, *145*(3), 833–855. https://doi.org/10.1175/MWR-D-16-0258.1

Lin, S.-J. (2004). A 'vertically Lagrangian' finite-volume dynamical core for global models. *Monthly Weather Review*, *132*, 2293–2307.

McRae, A. T. T., & Cotter, C. J. (2013). Energy- and enstrophy-conserving schemes for the shallow-water equations, based on mimetic finite elements. *Quarterly Journal of the Royal Meteorological Society*, *140*(684), 2223–2234. https://doi.org/10.1002/qj.2291

Medeiros, B., Williamson, D. L., & Olson, J. G. (2016). Reference aquaplanet climate in the Community Atmosphere Model, version 5. *Journal of Advances in Modeling Earth Systems*, *8*, 406–424. https://doi.org/10.1002/2015MS000593

Neale, R. B., Chen, C.-C., Gettelman, A., Lauritzen, P. H., Park, S., Williamson, D. L., et al. (2012). Description of the NCAR Community Atmosphere Model (CAM 5.0) (NCAR Technical Note NCAR/TN-486+STR). Boulder, CO: National Center of Atmospheric Research.

Neale, R. B., & Hoskins, B. J. (2000). A standard test for AGCMs including their physical parametrizations: I: The proposal. *Atmospheric Science Letters*, *1*(2), 101–107. https://doi.org/10.1006/asle.2000.0022

Skamarock, W. C., Klemp, J. B., Duda, M. G., Fowler, L., Park, S.-H., & Ringler, T. D. (2012). A multi-scale nonhydrostatic atmospheric model using centroidal Voronoi tesselations and C-grid staggering. *Monthly Weather Review*, *240*, 3090–3105. https://doi.org/10.1175/MWR-D-11-00215.1

Starr, V. P. (1945). A quasi-Lagrangian system of hydrodynamical equations. *Journal of the Atmospheric Sciences*, *2*, 227–237.

Taylor, M. A. (2011). Conservation of mass and energy for the moist atmospheric primitive equations on unstructured grids. In P. H. Lauritzen, R. D. Nair, C. Jablonowski, & M. Taylor (Eds.), *Numerical techniques for global atmospheric models, Lecture Notes in Computational Science and Engineering* (Vol. 80, pp. 357–380). Berlin: Springer. https://doi.org/10.1007/978-3-642-11640-7_12

Thuburn, J. (2008). Some conservation issues for the dynamical cores of NWP and climate models. *Journal of Computational Physics*, *227*, 3715–3730.

Trenberth, K. E., & Fasullo, J. T. (2018). Applications of an updated atmospheric energetics formulation. *Journal of Climate*, *31*(16), 6263–6279. https://doi.org/10.1175/JCLI-D-17-0838.1

Wan, H., Rasch, P. J., Taylor, M. A., & Jablonowski, C. (2015). Short-term time step convergence in a climate model. *Journal of Advances in Modeling Earth Systems*, *7*, 215–225. https://doi.org/10.1002/2014MS000368

Williamson, D. L. (2002). Time-split versus process-split coupling of parameterizations and dynamical core. *Monthly Weather Review*, *130*, 2024–2041.

Williamson, D. L., & Olson, J. G. (2003). Dependence of aqua-planet simulations on time step. *Quarterly Journal of the Royal Meteorological Society*, *129*(591), 2049–2064.

Williamson, D. L., Olson, J. G., Hannay, C., Toniazzo, T., Taylor, M., & Yudin, V. (2015). Energy considerations in the Community Atmosphere Model (CAM). *Journal of Advances in Modeling Earth Systems*, *7*, 1178–1188. https://doi.org/10.1002/2015MS000448

Zhang, K., Rasch, P. J., Taylor, M. A., Wan, H., Leung, R., Ma, P.-L., et al. (2018). Impact of numerical choices on water conservation in the E3SM atmosphere model version 1 (EAMv1). *Geoscientific Model Development*, *11*(5), 1971–1988. https://doi.org/10.5194/gmd-11-1971-2018